ELSEVIER

Chemical Engineering Journal 135S (2008) S99–S103

Chemical Engineering Journal

www.elsevier.com/locate/cej

Mesoporous silica films as catalyst support for microstructured reactors: Preparation and characterization

Oki Muraza [a], Evgeny V. Rebrov [a], Tetyana Khimyak [b], Brian F.G. Johnson [b], Patricia J. Kooyman [c], Ugo Lafont [c], Mart H.J.M. de Croon [a], Jaap C. Schouten [a,*]

[a] *Laboratory of Chemical Reactor Engineering, Eindhoven University of Technology, P.O. Box 513, 5600 MB Eindhoven, The Netherlands*
[b] *Department of Chemistry, University of Cambridge, Lensfield Road, Cambridge CB2 1EW, UK*
[c] *DelftChemTech/NCHREM, Delft University of Technology, Julianalaan 136, 2628 BL Delft, The Netherlands*

Abstract

Mesoporous silica thin films with hexagonal and cubic mesostructure have been deposited by the evaporation induced self-assembly assisted sol–gel route on microchannels etched in a Pyrex® 7740 borosilicate glass substrate. Prior to the synthesis, a 50 nm TiO_2 film has been deposited on the substrate by atomic layer deposition from titanium tetrachloride and water to increase adhesion of the mesoporous films to the walls of the substrate. The mesoporous films were produced by templating a silica precursor (TEOS) with the non-ionic surfactant Pluronic F127 ($EO_xPO_yEO_x$, EO, ethylene oxide; PO, propylene oxide; $x = 106$; $y = 70$). The effect of the channel aspect ratio on the uniformity of the silica films was investigated in the channels with a depth of 50 μm and with a width of 100–250 μm. Depending on the microchannel geometry, the thickness along the channels varies in the range of 0.3–1.0 μm. The most uniform films across the whole channel cross-section were obtained at the width-to-depth ratio of 3. Afterwards, the mesoporous films were impregnated with an ether–dichloromethane suspension of $[PPN]_2[Ru_{10}Pt_2C_2(CO)_{28}]$ mixed-metal cluster precursor to obtain well-dispersed, isolated and anchored bimetallic nanoparticles of 3–4 nm in diameter.

Keywords: Mesoporous silica films; Microchannel geometry; Thin film quality; EISA; Ru–Pt cluster

1. Introduction

Development in catalytic microreactor technology will be strongly promoted by a progress in techniques to incorporate very active catalyst films into microreactors [1]. Up to now, many catalyst supports are amorphous materials with a low surface area and non-structured porosity, usually developed by wash coating [2,3] and anodic oxidation techniques [3]. Microporous and mesoporous solid materials are the new generation of high surface area catalysts and catalyst supports, which can be used in microstructured reactors [4–8]. Mesoporous silica thin films with an ultrahigh specific surface area (800–1000 m^2/g) and a pore size in the range of 2–8 nm [9,10] can be deposited on the walls of microchannels to be used as a catalyst support in processing of large organic molecules, which are usually intermediates in the production of fine chemicals. The microreactors have to be preferably made in glass, because of its high intrinsic resistance to chemicals. Several deposition techniques have already been applied to obtain mesoporous coatings with either hexagonal or cubic mesostructures in microchannels: modified sol–gel synthesis [11,12], hydrothermal synthesis [13] and evaporation induced self-assembly (EISA) [14,15]. The effects of the composition of the initial solution and the aging time have been studied to find out the desired fraction of organic phase to modulate the reactivity of the precursors and to adjust preferential interactions at the organic/inorganic interface in subsequent self-assembly processes. However, film uniformity is less explored on microstructured substrates. The non-uniformity in the thickness of a catalytic coating increases the residence time distribution in a microreactor resulting in a lower conversion and selectivity. The non-uniformity with respect to the coating thickness should be below 2% of the open cross-sectional area of the microchannel [16]. This implies that very active catalysts have to be used in order to provide effective utilization of the reactor volume.

Supported bimetallic clusters are superior to their monometallic counterparts in selective hydrogenations [17–19]. There are several ways to prepare bimetallic heterogeneous catalysts on a surface. Co-impregnation of metal salts is the most common method to obtain bimetallic catalysts. The

* Corresponding author.
E-mail address: j.c.schouten@tue.nl (J.C. Schouten).

1385-8947/$ – see front matter © 2007 Elsevier B.V. All rights reserved.
doi:10.1016/j.cej.2007.07.023

main drawback of this method is a large variation in the size, morphology and stoichiometry of the resulting nanoparticles, since there is hardly any control of the structure and composition during the subsequent reduction step. On the contrary, mixed-metal cluster impregnation provides a good control of both size and composition. In this method, the bimetallic cluster precursors are adsorbed on the support from a suspension and activated by removal of the ligands with gentle thermolysis [20–22]. Coalescence and sintering of the nanoparticles is prevented by firmly anchoring them to the support. Therefore, it is important that the support has a high concentration of the functional groups on the surface to accommodate the nanoparticles.

Our previous work [23] was focused on the development of a method to deposit thin silica films on the flat borosilicate glass substrates using triblock copolymer Pluronic F127 ($EO_{106}PO_{70}EO_{106}$, EO, ethylene oxide; PO, propylene oxide) as structure directing agent. The destabilization of the sol was done by an EISA method in a spin-coater for 30 s to form an intermediate hybrid material [14,15]. Complete solvent removal was not achieved in the spinning rate range 500–1400 rpm. However, the thicknesses of the films obtained in the 2000–2500 rpm were in the range of 300–500 nm. A F127/silica ratio of 0.0076 and a spinning rate of 1500 rpm were found to be optimal to obtain the films with a surface area above 500 m^2/g and a monomodal pore size distribution with a mean pore size between 6.9 and 8.2 nm [23]. In the present study, this method was adapted to the deposition of thin films in semi-oval microchannels with a depth of 50 μm. The effect of the channel aspect ratio on the uniformity of the silica films was investigated in the channels with a width of 100, 150, 200 and 250 μm. These mesostructured films were then impregnated with a Pt–Ru mixed metal cluster to obtain the active catalysts. By this approach, the functionality of the relatively fragile bimetallic clusters is mediated through the rigid inorganic framework providing protection and the 3D distribution of the catalytic function. The resulting films can be used in a number of fine chemicals synthesis reactions.

2. Experimental

2.1. Synthesis of catalytic films

The preparation method includes three major steps: substrate modification, preparation of the mesoporous silica films and catalyst deposition (Scheme 1). A straight microchannel with a depth of 50 μm and a semi-oval cross-section was etched in a Pyrex® 7740 borosilicate glass substrate (20 mm length, 10 mm width and 0.5 mm thickness). The channels with widths of 100, 150, 200 and 250 μm were produced by wet etching. The surface roughness of the substrates was increased to 500 nm by a micropowder jet treatment [24] to prevent crack formation in the film layer during subsequent temperature excursions. A 50 nm TiO_2 layer was deposited by atomic layer deposition (ALD) from titanium tetrachloride and water to improve adhesion of the films to the substrate surface. Just before the synthesis, the titania layer was made super hydrophilic (>15 OH groups/nm^2) by an UV treatment [25].

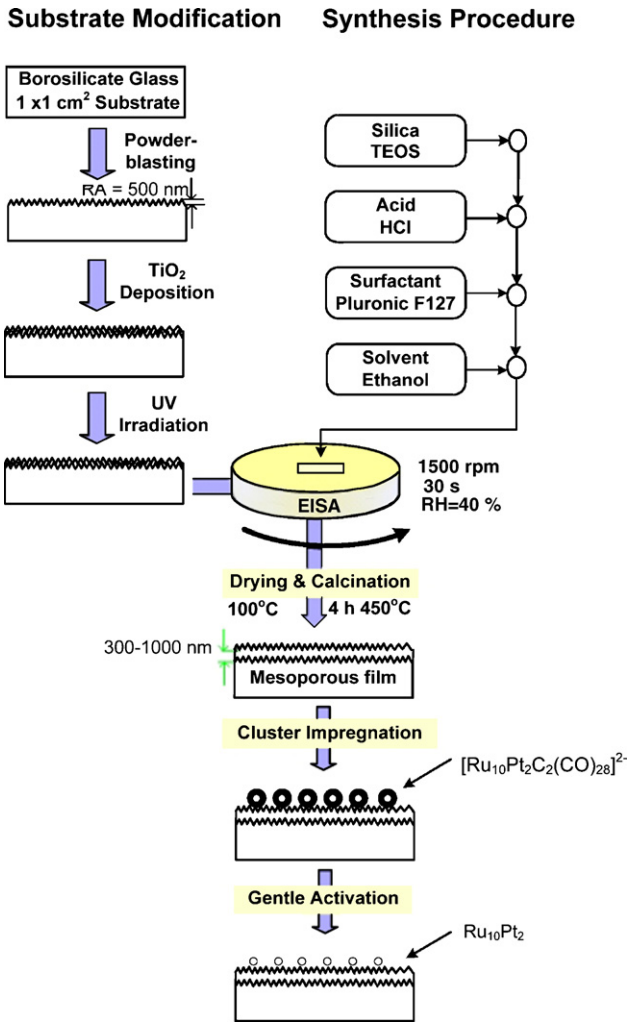

Scheme 1. Method for preparation of mesoporous catalytic films on a substrate.

The sol molar composition was: 1.0 TEOS:0.0055–0.0076 Pluronic F127:5.60 ethanol:5.03 H_2O. The details of the preparation procedure are reported in ref. [23].

The molecular cluster $[PPN]_2[Ru_{10}Pt_2C_2(CO)_{28}]$ (PPN = bis(triphenylphosphane)iminium) was used as a precursor for nanostructured catalysts [21,22]. Four substrate plates with deposited mesoporous films were fixed in a holder and then immersed in an ether–dichloromethane suspension (20 ml ether and 10 drops of dichloromethane) containing 10 mg (2.8 μmol) of the precursor for 4 days. Then the plates were washed with diethylether and dried in vacuum. The impregnated plates were subsequently heated in vacuum at 180 °C to decarbonylate the molecular cluster leading to the formation of anchored bare metallic nanoparticles.

2.2. Characterization

Phase composition was determined by X-ray diffraction in the range of 0.5–4° 2θ, using step scanning at 0.02° 2θ per step size and a counting time of 1 or 10 s for each step. XRD data were collected on a Rigaku Geigerflex Max/B diffractometer (40 kV, 40 mA) with Cu Kα radiation. Ethanol adsorption/desorption

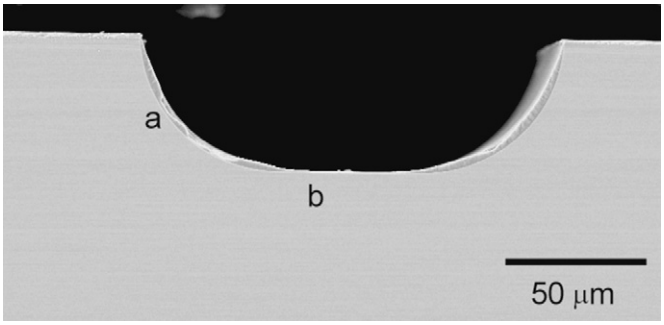

Fig. 1. FEG-SEM image of the cross-section of the microchannel after film deposition. The sol composition was: 1.0 TEOS:0.0076 Pluronic T127:5.60 ethanol:5.03 H2O. Spinning rate: 1500 rpm.

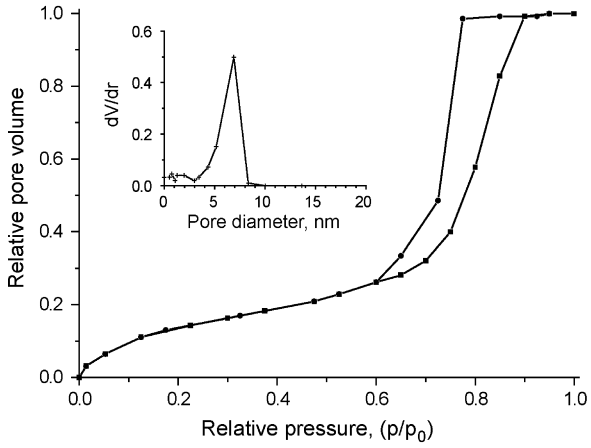

Fig. 3. Ethanol adsorption (■) and desorption (●) isotherms and pore size distribution plot. The sol composition was the same as that in Fig.1.

isotherms were recorded by ellipsometric porosimetry (EP) to determine pore-size distribution in the films. This method measures the changes of the optical characteristics of the porous film during vapor adsorption and desorption. Prior to adsorption, the samples were treated at 300 °C and a residual pressure of 0.1 mbar for 30 min to remove all adsorbed species. Then, the temperature was decreased to 14 °C and the ethanol partial pressure was increased stepwise to 40 mbar. The details of the EP experiments are described elsewhere [23]. The morphology of the films was determined by high resolution transmission electron microscopy (HR-TEM). HR-TEM was performed using a Philips CM30T microscope equipped with a LaB_6 filament and operated at 250 kV or a Philips CM30UT microscope equipped with a FEG operated at 300 kV. The particle size distribution (PSD) was obtained by measuring 100 particles from the HR-TEM micrographs. The mean particle diameter was calculated by the following formula: $d_m = (1/100)\sum_{i=1}^{100} n_i d_i$, where n_i is the number of particles with diameter d_i.

The morphology of the films was studied by a field-emission gun scanning electron microscope (FEG-SEM, Philips SEM XL40 FEG) and a laser scanning confocal microscope (LSCM). The FEG-SEM was operated at 6 or 8 kV. For FEG-SEM, the samples were glued to the sample holder with a carbon tape and sputtered with platinum. FEG-SEM images of the cross-section of the microchannel were taken at the side and at the bottom wall to study the uniformity of the film layer (Fig. 1).

3. Results and discussion

Mesoporous silica films with hexagonal and cubic mesostructures can be prepared on borosilicate glass substrates by the EISA assisted sol–gel route at different surfactant to silica ratios, pH and aging times [23]. Regular long-order mesostructured silica films with an average pore size of 8.2 nm are observed in the HR-TEM images (Fig. 2). The films have 3D cubic *Im*3*m* symmetry with a unit cell parameter (a_0) of 15.9 nm.

Typical ethanol adsorption–desorption isotherms are shown in Fig. 3. The sample exhibits a type IV isotherm with a hysteresis loop and a narrow pore size distribution. The mean pore size is 6.9 nm. The total pore volume is 0.3 cm^3/g. Those data are close to reported in literature (6.5 nm and 0.45 cm^3/g) for F127 templated mesoporous silica films [9].

To investigate the influence of channel geometry on the film quality, the width to depth ratio (t) of the microchannel is varied between 2 and 5. Typical FEG-SEM images of channel cross-

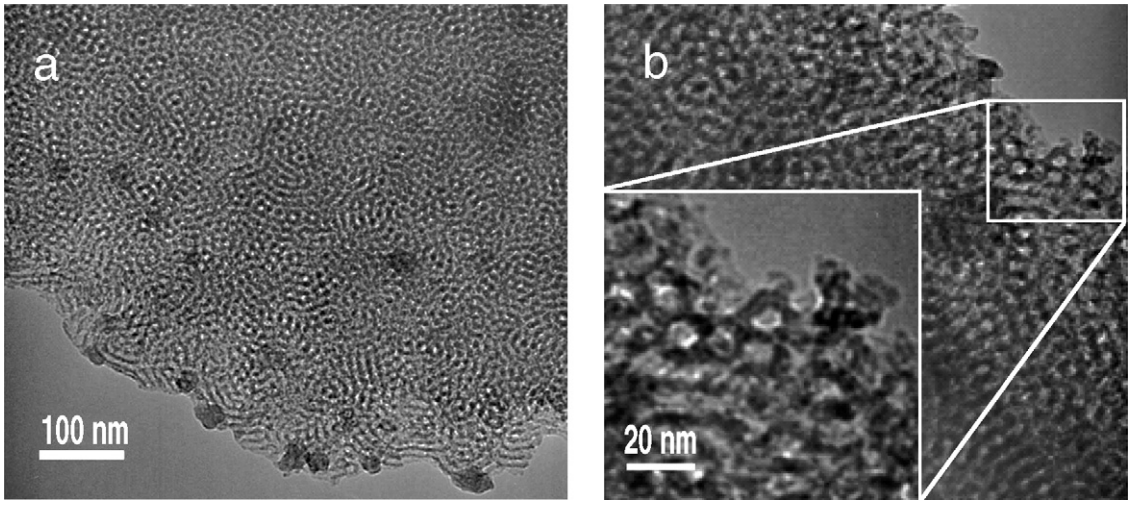

Fig. 2. HR-TEM images of highly ordered mesoporous silica films at different magnifications. The synthesis conditions were the same as those in Fig. 1.

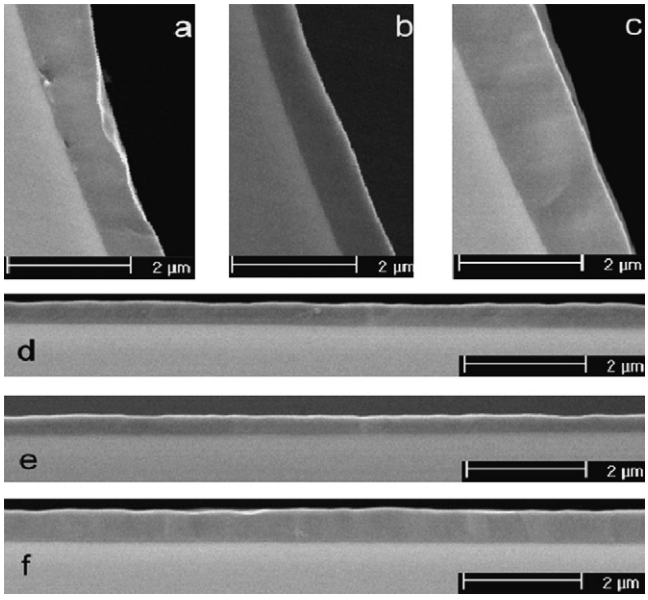

Fig. 4. Cross-sectional FEG-SEM image of highly ordered silica films on a microchannel with an aspect ratio of 2 (a, d); 3 (b, e) and 5 (c, f). The sol composition was the same as that in Fig. 1.

sections with deposited mesoporous silica films are shown in Fig. 4. One can see that a continuous film was obtained in all cases. However, the thickness of the film on the side walls is always larger than that on the bottom wall of the microchannel (Table 1). The silica film at the side walls is the thickest (1.40 ± 0.04 μm) on the channel with the width-to-depth ratio of 5. The largest difference in the film thickness between the side and bottom walls (h factor) of ca. 2.4 is also observed at this aspect ratio. Within the limitations of this study (one spinning rate and one sol composition), there is only little difference in film thickness between the microchannels with $t = 2$ and 3. In both cases, thinner films are obtained both on the side and the bottom walls. A two-fold difference in the coating thickness is considered to be reasonable for this particular channel geometry. An uneven distribution of coating thickness in the microchannels was previously reported after washcoating [2] and sol–gel routes [26]. Generally, the larger channel depth to width ratio, the higher the difference in coating thickness. A two- to three-fold difference in film thickness between the side and bottom walls of microchannels is reported [2] with the thickest film always at the bottom. The situation is opposite when the spin-coating method is applied. The thickness of the film is always lower at

Table 1
The thickness of mesoporous silica films at different aspect ratios of the microchannel cross-section

t	Film thickness, μm				$\frac{\bar{h}_s}{\bar{h}_b}$
	Side wall (h_s)		Bottom wall (h_b)		
	Minimum	Maximum	Minimum	Maximum	
2	0.79	1.00	0.40	0.45	2.1
3	0.67	0.78	0.36	0.37	2.0
5	1.36	1.44	0.58	0.59	2.4

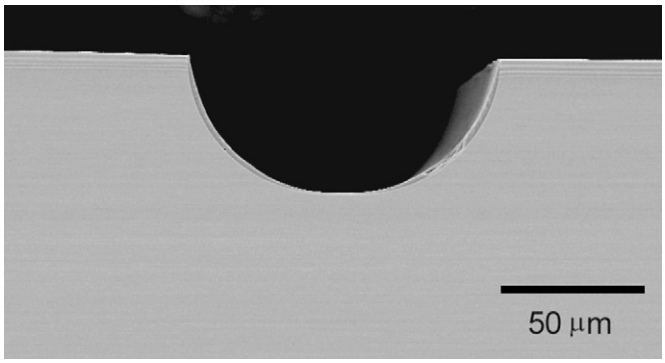

Fig. 5. Cross-sectional FE-SEM image of highly ordered silica films on a semicircular microchannel with a diaterer of 100 micron. The synthesis conditions are the same as those in Fig. 1.

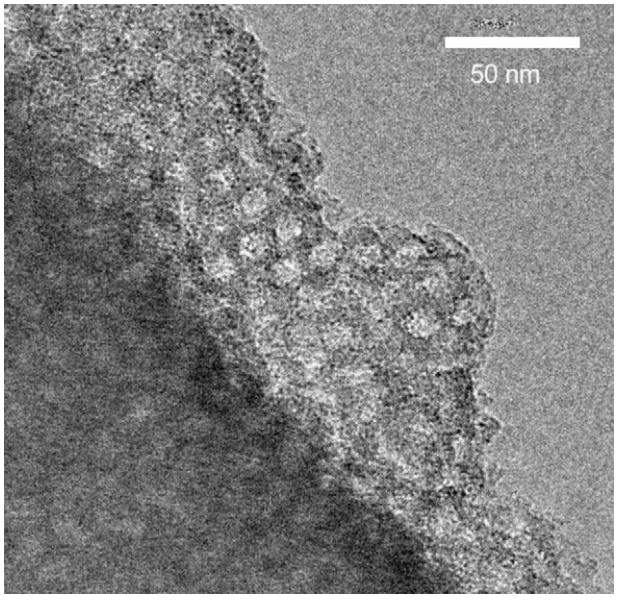

Fig. 6. HR-TEM image of Pt–Ru particles deposited on mesostructured films. The synthesis conditions are the same as those in Fig. 1.

the bottom of the microchannels. The film thickness is slightly larger for a semicircular channel ($t = 2$) as shown in Fig. 5.

The adhesion of mesoporous films to the substrate is high with a weight loss of less than 1 wt.% after 15 min ultrasonication. The XPS data (not shown) reveal the bimetallic character of the nanoparticles. After the encapsulation of the bimetallic clusters, HR-TEM images show the intact porosity which consists of randomly accessible ordered domains as well as the partly disordered mesostructure of silica films (Fig. 6). The Ru–Pt nanoparticles show a narrow particle size distribution. However, HR-TEM shows the agglomeration of nanoparticles into large clusters. The metal particles are 3–4 nm in diameter.

4. Conclusions

Mesoporous silica thin films with a thickness of 0.36–1.40 μm have been prepared by the evaporation induced self-assembly assisted sol–gel route on the microchannels etched in a Pyrex 7740 borosilicate glass substrate. The width to depth

ratio of the microchannels between 2 (semi-circular) and 3 (semi-oval) was found to provide the minimum non-uniformity of ca. 2 in the film thickness between the side and bottom walls of the microchannel. Well-dispersed, bimetallic $Ru_{10}Pt_2$ nanoparticles of 3–4 nm have been successfully introduced into the mesoporous films. The intact long-order porosity with a pore size of 8.2 nm after the encapsulation of the bimetallic clusters was observed.

Acknowledgements

The authors would like to thank Dr. M. Putkonen from Helsinki University of Technology and M. Vervest from Philips Material Analysis for ALD of titania films and the FEG-SEM measurements, respectively. The financial support by the Dutch Technology Foundation (STW, project no. EPC.6359), Organon, DSM, Shell, Akzo Nobel Chemicals, Bronkhorst, and TNO is gratefully acknowledged. BASF Europe is acknowledged for providing surfactant Pluronic F127.

References

[1] V. Hessel, S. Hardt, H. Lowe, Chemical Micro Process Engineering, Fundamentals, Modeling and Reactions, Wiley-VCH, Weinheim, 2004.
[2] R. Zapf, C. Becker-Willinger, K. Berresheim, H. Bolz, H. Gnazer, V. Hessel, G. Kolb, P. Lob, A.-K. Pannwitt, A. Ziogas, Trans. IChemE Part A 81 (2003) 721–729.
[3] M.A. Liauw, M. Baerns, R. Broucek, O.V. Buyevskaya, J.-M. Commenge, J.-P. Corriou, K. Gebauer, H.-J. Hefter, O.-U. Langer, M. Matlosz, A. Renken, A. Rouge, R. Schenk, N. Steinfeldt, St. Walter, Periodic operation in microchannel reactors, in: W. Ehrfeld (Ed.), Proc. Microreaction Technology: 3rd Int. Conf. on Microreaction Technology, Springer, Berlin, 2000, pp. 224–234.
[4] C.T. Kresge, M.E. Leonowicz, W.J. Roth, J.C. Vartuli, J.S. Beck, Nature 359 (1992) 710–712.
[5] J.S. Beck, J.C. Vartuli, W.J. Roth, M.E. Leonowicz, C.T. Kresge, K.D. Schmitt, C.T. Chu, D.H. Olson, E.W. Sheppard, S.B. McCullen, J.B. Higgins, J.L. Schlenker, J. Am. Chem. Soc. 114 (1992) 10834–10843.
[6] D. Zhao, J. Feng, Q. Huo, N. Melosh, G. Fredrickson, B. Chmelka, G. Stucky, Science 279 (1998) 548–552.
[7] D. Zhao, Q. Huo, J. Feng, B. Chmelka, G. Stucky, J. Am. Chem. Soc. 120 (1998) 6024–6036.
[8] J.M. Thomas, R. Raja, Stud. Surf. Sci. Catal. 148 (2004) 163–211.
[9] D. Zhao, P. Yang, N. Melosh, J. Feng, B. Chmelka, G. Stucky, Adv. Mater. 10 (1998) 1380–1385.
[10] D. Grosso, F. Cagnol, G.J.D.A.A. Soler-Illia, E.L. Crepaldi, H. Amenitsch, A. Brunet-Bruneau, A. Bourgeois, C. Sanchez, Adv. Funct. Mater. 14 (2004) 309–322.
[11] K. Haas-Santo, M. Fichtner, K. Schubert, Appl. Catal. A: Gen. 220 (2001) 79–92.
[12] H. Chen, L. Bednarova, R.S. Besser, W.Y. Lee, Appl. Catal. A: Gen. 286 (2005) 186–195.
[13] E.V. Rebrov, G.B.F. Seijger, H.P.A. Calis, M.H.J.M. de Croon, C.M. van den Bleek, J.C. Schouten, Appl. Catal. A: Gen. 206 (2001) 125–143.
[14] C.J. Brinker, Evaporation-induced self-assembly: functional nanostructures made easy, MRS Bull. 29 (2004) 631–640.
[15] M. Klotz, P.-A. Albouy, A. Ayral, C. Ménager, D. Grosso, A. Van der Lee, V. Cabuil, F. Babonneau, C. Guizard, Chem. Mater. 12 (2000) 1721–1728.
[16] E.R. Delsman, M.H.J.M. de Croon, G.D. Elzinga, P.D. Cobden, G.J. Kramer, J.C. Schouten, Chem. Eng. Technol. 28 (2005) 367–375.
[17] B.F.G. Johnson, Top. Catal. 24 (2003) 147–159.
[18] R. Raja, T. Khimyak, J.M. Thomas, S. Hermans, B.F.G. Johnson, Angew Chem. Int. Ed. 40 (2001) 4638–4642.
[19] W. Zhou, J.M. Thomas, D.S. Shephard, B.F.G. Johnson, D. Ozkaya, T. Maschmeyer, R.G. Bell, Q. Ge, Science 280 (1998) 705–708.
[20] S. Hermans, T. Khimyak, B.F.G. Johnson, J. Chem. Soc., Dalton Trans. 22 (2001) 3295–3302.
[21] B.F.G. Johnson, S. Hermans, T. Khimyak, Eur. J. Inorg. Chem. (2003) 1325–1331.
[22] T. Khimyak, B.F.G. Johnson, S. Hermans, A.D. Bond, Dalton Trans. 13 (2003) 2651–2657.
[23] O. Muraza, E.V. Rebrov, T. Khimyak, B.F.G. Johnson, P.J. Kooyman, U. Lafont, P.-A. Albouy, M.H.J.M. de Croon, J.C. Schouten, Stud. Surf. Sci. Catal. 162 (2006) 167–174.
[24] H. Yagyu, K. Sugano, S. Hayashi, O. Tabata, J. Micromech. Microeng. 15 (2005) 1236–1241.
[25] R. Wang, K. Hashimoto, A. Fujishima, M. Chikuni, E. Kojima, A. Kitamura, M. Shimohigoshi, T. Watanabe, Nature 388 (1997) 431–432.
[26] G. Germani, P. Alphonse, M. Courty, Y. Schuurman, C. Mirodatos, Catal. Today 110 (2005) 114–120.